J|A|C|S
ARTICLES
Published on Web 01/04/2006

Guest Exchange Dynamics in an M_4L_6 Tetrahedral Host§

Anna V. Davis,† Dorothea Fiedler,† Georg Seeber,† Achim Zahl,‡ Rudi van Eldik,‡ and Kenneth N. Raymond*,†

Contribution from the Department of Chemistry, University of California, Berkeley, California 94720-1460, and Institute for Inorganic Chemistry, University of Erlangen-Nürnberg, Egerlandstrasse 1, 91058 Erlangen, Germany

Received September 30, 2005; E-mail: raymond@socrates.berkeley.edu

Abstract: Guest exchange in an M_4L_6 supramolecular assembly was previously demonstrated to proceed through a nonrupture mechanism in which guests squeeze through apertures in the host structure and not through larger portals created by partial assembly dissociation. Focusing on the $[Ga_4L_6]^{12-}$ assembly {L = 1,5-bis(2′,3′-dihydroxybenzamido)naphthalene}, the host−guest kinetic behavior of this supramolecular capsule is defined. Guest self-exchange rates at varied temperatures and pressures were measured to determine activation parameters, revealing negative $\Delta S^{\ddagger}$ and positive $\Delta V^{\ddagger}$ values {PEt_4^+: $\Delta H^{\ddagger} = 74(3)$ kJ mol^{-1}, $\Delta S^{\ddagger} = -46(6)$ J mol^{-1} K^{-1}, $k_{298} = 0.003$ s^{-1}; NEt_4^+: $\Delta H^{\ddagger} = 69(2)$ kJ mol^{-1}, $\Delta S^{\ddagger} = -52(5)$ J mol^{-1} K^{-1}, $k_{298} = 0.009$ s^{-1}; $NMe_2Pr_2^+$: $\Delta H^{\ddagger} = 52(2)$ kJ mol^{-1}, $\Delta S^{\ddagger} = -56(7)$ J mol^{-1} K^{-1}, $\Delta V^{\ddagger} = +13(1)$ cm^3 mol^{-1}, $k_{298} = 4.4$ s^{-1}; NPr_4^+: $\Delta H^{\ddagger} = 42(1)$ kJ mol^{-1}, $\Delta S^{\ddagger} = -102(4)$ J mol^{-1} K^{-1}, $\Delta V^{\ddagger} = +31(2)$ cm^3 mol^{-1}, $k_{298} = 1.4$ s^{-1}}. In PEt_4^+ for NEt_4^+ exchange reactions, egress of the initial guest (G1) is found to be rate determining, with increasing G1 and G2 (the displacing guest) concentrations inhibiting guest exchange. This inhibition is explained by the decreased flexibility of the host imparted by exterior, or exohedral, guest interactions by both the G1 and G2 guests. Blocking the exohedral host sites with high concentrations of the smaller NMe_4^+ cation (a weak endohedral guest) enhances PEt_4^+ for NEt_4^+ guest exchange rates. Finally, guest displacement reactions also demonstrate the sensitivity of guest exchange to thermodynamic endohedral guest binding affinities. When the initial guest (G1) has a weaker affinity for the host, G2 concentration dependence is observed in addition to dependence on the G2 binding strength.

Introduction

The host−guest chemistry of discrete molecular capsules enables an array of molecular technologies based on the selective sequestration of chemical species in solution.[1−4] These applications include chemical sensing, molecular separations, reactive intermediate isolation, and encapsulated reaction chemistry. The construction of large, more complex container molecules from the self-assembly of smaller, programmed components has spurred the discovery of new host−guest phenomena, largely focused on the manipulation of chemical reactivity through encapsulation.[3−10] Host−guest dynamics are particularly relevant as a chemical transformation is transferred from the bulk solution into the "inner phase" of a molecular capsule.[2,11] The design of a catalytically active capsule, for example, requires a balance of the rates of guest exchange of the substrate, intermediates,

† University of California.

‡ University of Erlangen-Nürnberg.

§ Paper No. 33 in the series Coordination Number Incommensurate Cluster Formation. For the previous series paper see ref 24.

(1) Vriezema, D. M.; Aragonès, M. C.; Elemans, A. A. W.; Cornelissen, J. J. L. M.; Rowan, A. E.; Nolte, R. J. M. *Chem. Rev.* **2005**, *105*, 1445−1489. Rebek, J., Jr. *Angew. Chem., Int. Ed.* **2005**, *44*, 2068−2078. Steed, J. W.; Atwood, J. L. *Supramolecular Chemistry*; John Wiley & Sons: Ltd.: Chichester, 2000. Cram, D. J.; Cram, J. M. *Science* **1974**, *183*, 803−809. Lehn, J.-M. *Supramolecular Chemistry: Concepts and Perspectives*; VCH: Weinheim, 1995. Warmuth, R. *J. Inclusion Phenom.* **2000**, *37*, 1−38. Rudkevich, D. M. *Bull. Chem. Soc. Jpn.* **2002**, *75*, 393−413. Warmuth, R. *Eur. J. Org. Chem.* **2001**, 423−437. Pinalli, R.; Suman, M.; Dalcanale, E. *Eur. J. Org. Chem.* **2004**, 451−462.

(2) Cram, D. J. *Nature* **1992**, *356*, 29−36.

(3) Hof, F.; Craig, S. L.; Nuckolls, C.; Rebek, J., Jr. *Angew. Chem., Int. Ed.* **2002**, *41*, 1488−1508.

(4) Fiedler, D.; Leung, D. H.; Bergman, R. G.; Raymond, K. N. *Acc. Chem. Res.* **2005**, *38*, 351−360. Lützen, A. *Angew. Chem., Int. Ed.* **2005**, *44*, 1000−1002.

(5) Kang, J.; Rebek, J., Jr. *Nature* **1997**, *385*, 50−52. Kang, J.; Santamaría, J.; Hilmersson, G.; Rebek, J., Jr. *J. Am. Chem. Soc.* **1998**, *120*, 7389−7390. Kang, J.; Hilmersson, G.; Santamaría, J.; Rebek, J., Jr. *J. Am. Chem. Soc.* **1998**, *120*, 3650−3656.

(6) Körner, S. K.; Tucci, F. C.; Rudkevich, D. M.; Heinz, T.; Rebek, J., Jr. *Chem.—Eur. J.* **2000**, *6*, 187−195. Kusukawa, T.; Nakai, T.; Okano, T.; Fujita, M. *Chem. Lett.* **2003**, *32*, 284−285. Merlau, M. L.; Mejia, M. P.; Nguyen, S. T.; Hupp, J. T. *Angew. Chem., Int. Ed.* **2001**, *40*, 4239−4242. Wash, P. L.; Renslo, A. R.; Rebek, J., Jr. *Angew. Chem., Int. Ed.* **2001**, *40*, 1221−1222. Yoshizawa, M.; Kusukawa, T.; Fujita, M.; Yamaguchi, K. *J. Am. Chem. Soc.* **2000**, *122*, 6311−6312. Yoshizawa, M.; Kusukawa, T.; Fujita, M.; Sakamoto, S.; Yamaguchi, K. *J. Am. Chem. Soc.* **2001**, *123*, 10454−10459. Yoshizawa, M.; Takeyama, Y.; Kusukawa, T.; Fujita, M. *Angew. Chem., Int. Ed.* **2002**, *41*, 1347−1349. Yoshizawa, M.; Takeyama, Y.; Okano, T.; Fujita, M. *J. the Am. Chem. Soc.* **2003**, *125*, 3243−3247. Yoshizawa, M.; Miyagi, S.; Kawano, M.; Ishiguro, K.; Fujita, M. *J. Am. Chem. Soc.* **2004**, *126*, 9172−9173. Chen, J.; Körner, S.; Craig, S. L.; Lin, S.; Rudkevich, D. M.; Rebek, J., Jr. *Proc. Natl. Acad. Sci. U.S.A.* **2002**, *99*, 2593−2596.

(7) Ziegler, M.; Brumaghim, J. L.; Raymond, K. N. *Angew. Chem., Int. Ed.* **2000**, *39*, 4119−4121. Brumaghim, J. L.; Michels, M.; Raymond, K. N. *Eur. J. Org. Chem.* **2004**, 4552−4559.

(8) Brumaghim, J. L.; Michels, M.; Pagliero, D.; Raymond, K. N. *Eur. J. Org. Chem.* **2004**, 5115−5118.

(9) Leung, D. H.; Fiedler, D.; Bergman, R. G.; Raymond, K. N. *Angew. Chem., Int. Ed.* **2004**, *43*, 963−966.

(10) Fiedler, D.; Bergman, R. G.; Raymond, K. N. *Angew. Chem., Int. Ed.* **2004**, *43*, 6748−6751.

(11) Davis, A. V.; Yeh, R. M.; Raymond, K. N. *Proc. Natl. Acad. Sci., U.S.A.* **2002**, *99*, 4793−4796.

 10.1021/ja056556+ CCC: $33.50

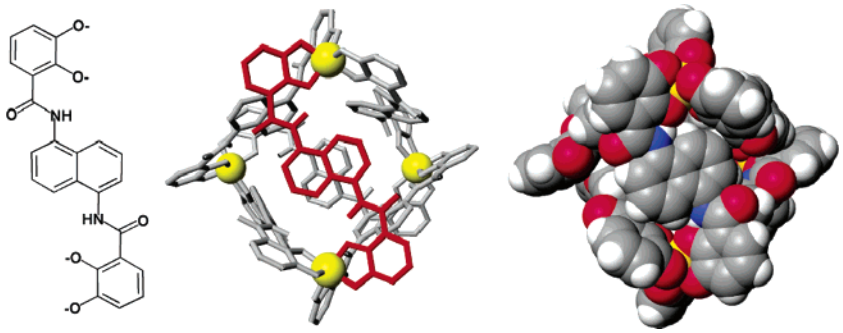

Figure 1. (Left) L^{4-} ligand. (Middle and Right) Wire-frame and space-filling views down the 2-fold axis of the $[Fe_4L_6]^{12-}$ crystal structure.[19]

and product with the rate of the chemical transformation itself.[5,10] Alternatively, differences in host−guest dynamics may be exploited to influence substrate specificity.[9]

Self-assembled hosts differ greatly in their structures and chemical composition and isolate their encapsulated cargo from the bulk solution to varying degrees. The lowest energy guest exchange pathway will depend on both the lability of assembly components and the size of accessible portals or apertures in the host frame, and a number of mechanistic studies have been reported demonstrating the variety of guest exchange pathways.[12−16] Among capsules assembled from hydrogen-bonding components, for example, guest exchange has been found to require only partial disruption of a hydrogen-bonding seam in some systems[12,13] and complete capsule dissociation in others.[15] For less labile metal−ligand structures, facile guest exchange may require the design of larger host portals.[17]

We have recently described the mechanism of guest exchange in a supramolecular host assembled from metal and ligand components, demonstrating that guest exchange does not involve partial dissociation or rupture of the host structure.[18] This finding has direct bearing on the known encapsulated reaction chemistry of the host and provides direction for both the development of new encapsulated reactions and the design of new host reactors.[4,7−10] Here we expand on our initial report and reveal the sensitivity of host dynamics to exterior, or exohedral, guests, and to guest binding affinities, and we define activation parameters for guest exchange.

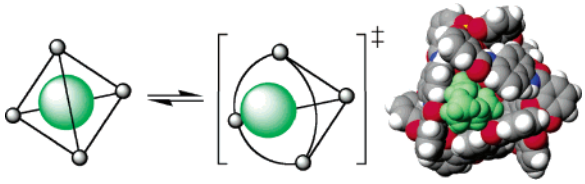

Figure 2. Guest exchange in the M_4L_6 host proceeds through a nondissociative mechanism in which an aperture in the host structure enlarges to accommodate guest passage. A transition state model for a NEt_4^+ guest is shown.[18,25]

Results and Discussion

We have previously reported the self-assembly of an M_4L_6 host from six bis-bidentate catecholamide ligands and four pseudo octahedral metal ions (Figure 1, L = 1,5-bis(2′,3′-dihydroxybenzamido)naphthalene).[19−21] The chiral, *T*-symmetric structure binds a variety of small molecules,[8,19,20,22,23] generally encapsulating monocationic species, and structural evidence supports the conclusion that encapsulated species are well-isolated from the bulk solution. Guests range in size from tetramethylammonium[19] to decamethylcobaltacinium[18] and in chemical reactivity from inert alkylammonium ions[19,20,22] to Ir^{III} organometallic complexes capable of C−H activation.[9] The small-molecule binding properties of the assembly have been extended to encapsulated reaction chemistry, effecting the stabilization of reactive phosphonium−ketone adducts,[7] and modulating the C−H activation reactivity of an encapsulated Ir catalyst.[9] M_4L_6 encapsulation of enammonium substrates leads to dramatic acceleration (up to 1000-fold) of the aza-Cope rearrangement and an encapsulated catalytic cycle capable of multiple turnovers.[10]

Recently, we described a mechanism of guest exchange for the M_4L_6 host, concluding that the host deforms to enlarge an aperture for guest egress and ingress, instead of rupturing an M−L chelate attachment to create a portal for guest passage.[18] The host possesses four symmetrically equivalent apertures at the intersection of three ligands opposite to each C_3 symmetric metal vertex, and molecular modeling studies indicate that the host is elastic enough to access the requisite aperture dilation for guest exchange (Figure 2). In addition to the modeling results, the findings that the lability of host components did not impact guest exchange rates and that a severely sterically

(12) Szabo, T.; Hilmersson, G.; Rebek, J., Jr. *J. Am. Chem. Soc.* **1998**, *120*, 6193−6194. Craig, S. L.; Lin, S.; Chen, J.; Rebek, J., Jr. *J. Am. Chem. Soc.* **2002**, *124*, 8780−8781.
(13) Santamaría, J.; Martín, T.; Hilmersson, G.; Craig, S. L.; Rebek, J., Jr. *Proc. Natl. Acad. Sci. U.S.A.* **1999**, *96*, 8344−8347.
(14) Ibukuro, F.; Kusukawa, T.; Fujita, M. *J. Am. Chem. Soc.* **1998**, *120*, 8561−8562. Tominaga, M.; Tashiro, S.; Aoyagi, M.; Fujita, M. *Chem. Commun.* **2002**, 2038−2039. Fox, O. D.; Dalley, N. K.; Harrison, R. G. *J. Am. Chem. Soc.* **1998**, *120*, 7111−7112. Fox, O. D.; Dalley, N. K.; Harrison, R. G. *Inorg. Chem.* **1999**, *38*, 5860−5863. Hof, F.; Nuckolls, C.; Craig, S. L.; Martín, T.; Rebek, J., Jr. *J. Am. Chem. Soc.* **2000**, *122*, 10991−10996. Kerckhoffs, J. M. C. A.; van Leeuwen, F. W. B.; Spek, A. L.; Kooijman, H.; Crego-Calama, M.; Reinhoudt, D. N. *Angew. Chem., Int. Ed.* **2003**, *42*, 5717−5722. Yamanaka, M.; Shivanyuk, A.; Rebek, J., Jr. *J. Am. Chem. Soc.* **2004**, *126*, 2939−2943. Vysotsky, M. O.; Bohmer, V. *Org. Lett.* **2000**, *2*, 3571−3574. Ro, S.; Rowan, S. J.; Pease, A. P.; Cram, D. J.; Stoddart, J. F. *Org. Lett.* **2000**, *2*, 2411−2414. Guest exchange has also been described for a host held together by dynamic covalent bonds: Cai, M.; Siderov, V.; Lam, Y.-F.; Flowers, R. A., II.; Davis, J. T. *Org. Lett.* **2000**, *2*, 1665−1668.
(15) Mogck, O.; Pons, M.; Böhmer, V.; Vogt, W. *J. Am. Chem. Soc.* **1997**, *119*, 5706−5712.
(16) Zuccaccia, D.; Pirondini, L.; Pinalli, R.; Dalcanale, E.; Macchioni, A. *J. Am. Chem. Soc.* **2005**, *127*, 7025−7032.
(17) Umemoto, K.; Tsukui, H.; Kusukawa, T.; Biradha, K.; Fujita, M. *Angew. Chem., Int. Ed.* **2001**, *40*, 2620−2622.
(18) Davis, A. V.; Raymond, K. N. *J. Am. Chem. Soc.* **2005**, *127*, 7912−7919.
(19) Caulder, D. L.; Powers, R. E.; Parac, T. N.; Raymond, K. N. *Angew. Chem., Int. Ed.* **1998**, *37*, 1840−1843.
(20) Caulder, D. L.; Brückner, C.; Powers, R. E.; König, S.; Parac, T. N.; Leary, J. A.; Raymond, K. N. *J. Am. Chem. Soc.* **2001**, *123*, 8923−8938.
(21) Caulder, D. L.; Raymond, K. N. *Acc. Chem. Res.* **1999**, *32*, 975−982.
(22) Parac, T. N.; Caulder, D. L.; Raymond, K. N. *J. Am. Chem. Soc.* **1998**, *120*, 8003−8004.

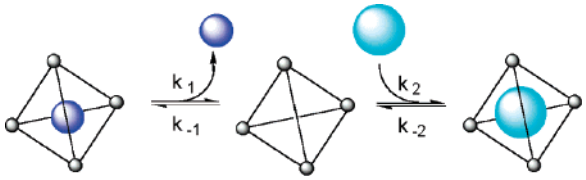

Figure 3. Dissociation of an initially bound guest (G1, smaller dark blue sphere) likely precedes its replacement by a second guest (G2, larger light blue sphere). The schematic does not imply that the "empty" host intermediate is necessarily free of encapsulated solvent.[13,28]

encumbered guest such as $CoCp^*_2{}^+$ inhibited guest exchange built a strong case for a nondissociative guest exchange mechanism. Furthermore, recent studies illustrated that the host structure can be permeated by a guest molecule's protruding tail (a long alkylsulfonate chain), while retaining its structural integrity.[24]

Encapsulated guest species in M_4L_6 tetrahedra are most easily identified by ^{1}H NMR, as the naphthyl moieties enclosing the host cavity magnetically shield the guest due to ring current effects.[19] This effect causes significant upfield shifting of the ^{1}H resonances of encapsulated species (several ppm), while resonances of the unencapsulated guest population appear further downfield. Initially bound guests (G1) in the M_4L_6 tetrahedra are readily displaced by more strongly binding guests (G2), and such exchange reactions can be observed by ^{1}H NMR.[18,19] Guests are known to exist in equilibrium between encapsulated and unencapsulated ("free") sites, and binding constants have been determined for a number of guests by ^{1}H NMR and calorimetry.[19,22,26,27] For a guest with a binding constant on the order of 10^4 M^{-1}, 13% of the host population will be "empty" (i.e., of guest)[28] in a 5 mM solution of the 1:1 host−guest complex and 0.1% in a system of 1:20 host−guest stoichiometry. Thus, guest exchange likely occurs through an "empty" host intermediate (Figure 3).[13,28]

Consistent with this picture of the guest exchange reaction, preliminary experiments suggested that guest exchange rates correlate with binding affinities. A weakly binding guest will be in equilibrium with a larger fraction of unbound guest and empty host. For example, the self-exchange of bound and "free" $NMe_4{}^+$ in D_2O causes broadening of the ^{1}H NMR signals at room temperature,[19] while broadening of the $NEt_4{}^+$ signals could not be achieved at temperatures as high as 100 °C.[20] Initial guest exchange experiments demonstrated that the displacement of $NMe_4{}^+$ by $NEt_4{}^+$ is too fast to monitor by ^{1}H NMR but that displacement of $NEt_4{}^+$ by $PEt_4{}^+$ takes place more slowly.

Guest Self-Exchange. Perhaps the simplest guest exchange reaction involves the interchange of the encapsulated and nonencapsulated populations of the same chemical species. This self-exchange reaction is represented schematically in Figure 4. Self-exchange has been observed by ^{1}H NMR coalescence behavior in the case of $NMe_4{}^+$[29] and by 2D ^{1}H EXSY NMR experiments in the case of $NEt_4{}^+$.[20]

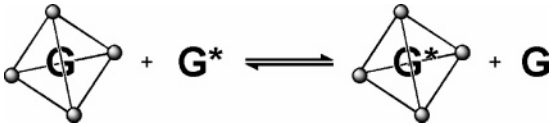

Figure 4. Self-exchange of chemically identical guests between encapsulated and unencapsulated sites can be followed by spin labeling (*) NMR experiments.

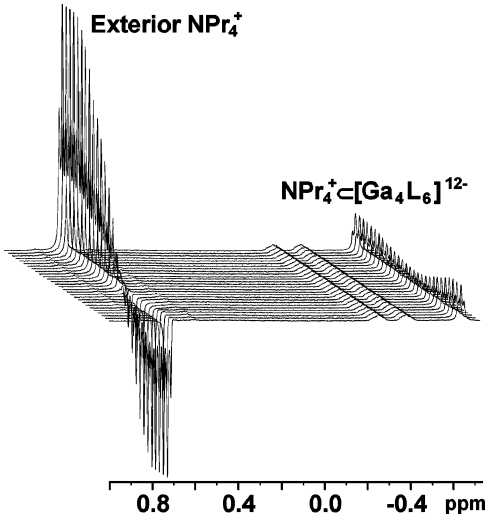

Figure 5. Exchange of free and $[Ga_4L_6]^{12-}$-encapsulated $NPr_4{}^+$ is observed by ^{1}H NMR selective inversion recovery. From the bottom spectrum to the top spectrum the delay between the selective inversion pulse and spectrum acquisition increases. The inverted spin population of the exterior CH_3 group is transferred to the encapsulated CH_3 resonance by chemical exchange, producing a dip in the resonance of the encapsulated CH_3 group.

A series of guests was chosen to further probe the relationship between self-exchange rates and guest binding affinities, and exchange was measured by the 1D selective inversion recovery (SIR) ^{1}H NMR experiment.[30] Inversion of the spin population of one resonance of the exchanging species is followed by a variable delay before acquisition of the 1D spectrum. The extent of chemical exchange between the inverted and noninverted populations (of the same chemical species) is related to the decrease in intensity of the exchange-related, noninverted resonance. SIR spectra for $NPr_4{}^+$ self-exchange in the $[Ga_4L_6]^{12-}$ are shown in Figure 5 in which the exterior $NPr_4{}^+$ methyl resonance (0.7 ppm) is selectively inverted. Exchange with the encapsulated $NPr_4{}^+$ population is evidenced by the dip in the intensity of its methyl resonance at intermediate delay times.

Selective inversion experiments were performed on $[Ga_4L_6]^{12-}$ samples containing $PEt_4{}^+$, $NEt_4{}^+$, $NMe_2Pr_2{}^+$, and $NPr_4{}^+$. For the $PEt_4{}^+$, $NEt_4{}^+$, and $NPr_4{}^+$ guests these measurements support the conclusion that guest self-exchange rates correlate with guest binding affinities, as increasing exchange rates are observed with decreasing binding affinities (Table 1). Thermodynamic ground state effects can account for the correlation of guest binding affinities with guest exchange rates, provided that guests share

(23) Parac, T. N.; Scherer, M.; Raymond, K. N. *Angew. Chem., Int. Ed.* **2000**, *39*, 1239−1242. Fiedler, D.; Pagliero, D.; Brumaghim, J. L.; Bergman, R. G.; Raymond, K. N. *Inorg. Chem.* **2004**, *43*, 846−848.
(24) Tiedemann, B. E.; Raymond, K. N. *Angew. Chem., Int. Ed.* **2006**, *45*, 83−86.
(25) *CAChe Workstation Pro*, 5.04; Fujitsu Limited: 2002.
(26) Parac, T. N.; Raymond, K. N. Unpublished results.
(27) Michels, M.; Raymond, K. N. Unpublished results.
(28) The "empty" host intermediate likely contains solvent (here water), although we have not been able to test this experimentally. As emphasized by a reviewer, the energetic penalties for complete desolvation of the host interior are probably quite large, and it is more plausible that the intermediate host is solvent filled. Throughout the manuscript, "empty" refers to the absence of the described guests and not the absence of solvent; we are not able to comment at this time on the role of encapsulated solvent in the guest exchange process. A distinct role of solvent in the guest exchange dynamics of hydrogen-bonded capsules has been demonstrated in another host−guest system: ref 13.
(29) Caulder, D. L. The Rational Design of Supramolecular Cluster. Ph.D. Thesis, University of California, Berkeley, CA, 1998.
(30) Perrin, C. L.; Dwyer, T. J. *Chem. Rev.* **1990**, *90*, 935−967. Bain, A.; Cramer, J. A. *J. Magn. Reson. A* **1993**, *103*, 217−222. Bain, A. D.; Cramer, J. A. *J. Magn. Reson. A* **1996**, *118*, 21−27.

Table 1. Guest Self-Exchange in $[Ga_4L_6]^{12-}$ [31]

guest	log $K_{binding}$ (298 K)	$\Delta H^{\ddagger}$ (kJ mol^{-1})	$\Delta S^{\ddagger}$ (J mol^{-1} K^{-1})	$\Delta G^{\ddagger}_{298}$ (kJ mol^{-1})	k_{298} (s^{-1})
PEt_4^+	5.0(2)	74(3)	−46(6)	78(4)	0.003
NEt_4^+	4.55(6)	69(2)	−52(5)	76(3)	0.009
$NMe_2Pr_2^+$	3.5(2)	52(2)	−56(7)	60(3)	4.4
NPr_4^+	2.0(2)	42(1)	−102(4)	63(3)	1.4

energetically similar transition states; strongly bound guests will be more stabilized relative to the transition state than weakly bound guests. However, the $NMe_2Pr_2^+$ exchange rate differs notably from this trend. While $NMe_2Pr_2^+$ has a significantly stronger thermodynamic affinity for the $[Ga_4L_6]^{12-}$ host than does NPr_4^+, it exchanges at a much faster rate.

In the initial report of M_4L_6 guest exchange mechanism, the relationship between guest size and exchange rate was exploited in testing the mechanism of guest exchange.[18] Decamethylcobaltacinium is such a large guest for the M_4L_6 assembly that it does not freely rotate within the host cavity but is instead trapped between two opposing ligand "walls," lowering the symmetry of the host from T to D_2. While NEt_4^+ can be displaced by an excess of PEt_4^+ within minutes at room temperature in water, $CoCp^*_2{}^+$ is completely entrapped, evidencing the limits of the host's elasticity. Unlike $CoCp^*_2{}^+$, the guests investigated here share greater malleability of their own structures, precluding clear relationships between size and exchange rates and allowing for greater influence of ground-state effects. In the case of $NMe_2Pr_2^+$, guest shape appears to be critical, with the streamlined (methyl groups first) conformation of $NMe_2Pr_2^+$ allowing for more facile passage through the host aperture than the bulkier NPr_4^+.

Measurement of guest exchange rates at different temperatures also allowed for the calculation of activation parameters by Eyring analysis (Table 1).[31] These values provide further insight into the exchange mechanism. The activation enthalpies follow the same trend as the guest binding constants, with higher $\Delta H^{\ddagger}$ values observed for more tightly binding guests. As a point of reference, the $\Delta H^{\ddagger}$ values are similar to, or lower than, those reported for the intramolecular, nonbond rupture stereoinversion reactions of mononuclear and dinuclear tris-catecholate Ga^{III} complexes (analogous to the metal centers of the $[Ga_4L_6]^{12-}$ host) in D_2O at basic pH,[32] bolstering the argument that metal−catecholate bonds of the $[Ga_4L_6]^{12-}$ are not broken in the exchange reaction. Similarly, the negative $\Delta S^{\ddagger}$ values are not indicative of bond rupture and instead appear to reflect the entropy cost in correctly orientating each guest for passage through the tight host aperture. This process likely involves conformational rearrangement of both the host and guest structures, as indicated by our modeling studies,[18] with the flexible guest cations being forced to adopt an especially streamlined configuration. Notably, the activation entropy for the largest guest, NPr_4^+, is much more negative than that of the other guests, reflecting the greater entropic cost for it to squeeze through the host aperture.[31] Such a large difference in $\Delta S^{\ddagger}$ values with guest size would not be anticipated if host rupture was required for guest exchange.

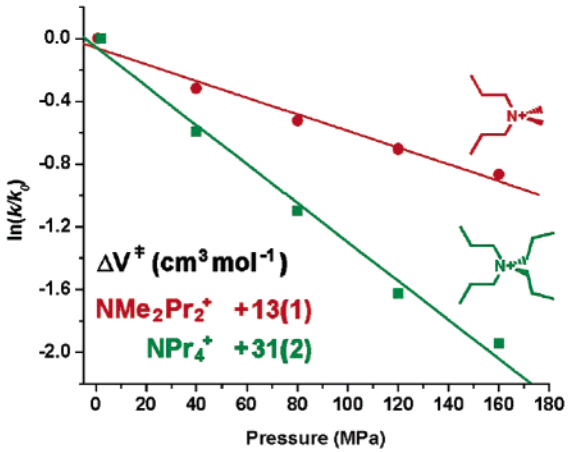

Figure 6. Exchange of both $NMe_2Pr_2^+$ and NPr_4^+ in $[Ga_4L_6]^{12-}$ are characterized by positive volumes of activation. Measurements were conducted in D_2O at basic pD, 30 °C, 5 mM host, and 6 equiv of guest.

Variation of the guest concentration in these experiments revealed a surprising result: guest exchange rates *decreased* with *increasing* guest concentration.[31] The extent of the inhibition varied depending on each guest, with $NMe_2Pr_2^+$ and NPr_4^+ demonstrating the largest inhibitory effects on their own exchange reactions.[33] As is expanded upon later, this phenomenon attests to the contribution of both interior *and* exterior guest interactions in the M_4L_6 system.

Variable pressure measurements allowed for determination of the volumes of activation for guest exchange, another test of the proposed mechanism.[34] If the guest has to squeeze through the host's aperture, a positive volume of activation is anticipated, and the pressure dependence should be more pronounced for sterically demanding guest molecules which cause a greater deformation in the transition state.[35] Selective inversion recovery experiments were conducted with the NPr_4^+ and $NMe_2Pr_2^+$ guests in the $[Ga_4L_6]^{12-}$ host in basic D_2O, at applied pressures ranging from 1 to 160 MPa. From these data volumes of activation were determined (Figure 6) from the relationship:

$$\Delta V^{\ddagger} = -RT(\partial \ln k/\partial P)_T \qquad (1)$$

The exchange reactions of both NPr_4^+ and $NMe_2Pr_2^+$ in the $[Ga_4L_6]^{12-}$ host are characterized by positive volumes of activation, reflective of the host deformation modeled for the nondissociative transition state. As a result of the deformation coupled to a volume increase, the dilated host transition state structure becomes less energetically accessible with increasing pressure. While solvation and counterion pairing effects make detailed interpretation of these values difficult, the difference

(31) The SIR samples used for the determination of activation parameters each contain 5 equiv of guest. In the determination of $\Delta S^{\ddagger}$, the pseudo-first-order k_{obs} values obtained from the SIR experiments were treated as first-order rate constants. If one assumes that the reaction order with respect to guest is −1, $\Delta S^{\ddagger}$ values are −82(6), −75(8), −130(5), and −86(6) J K^{-1} mol^{-1}, respectively, for PEt_4^+, NEt_4^+, NPr_4^+, and $NMe_2Pr_2^+$. The difference in treatment does not affect the determination of $\Delta H^{\ddagger}$ and $\Delta V^{\ddagger}$.

(32) Meyer, M.; Kersting, B.; Powers, R. E.; Raymond, K. N. *Inorg. Chem.* **1997**, *36*, 5179−5191. Kersting, B.; Telford, J. R.; Meyer, M.; Raymond, K. N. *J. Am. Chem. Soc.* **1996**, *118*, 5712−5721.

(33) It is likely that some rearrangement of the exterior ion-paired guests occurs as the host aperture dilates for guest exchange, and this process may contribute to the negative entropy of activation observed for the self-exchange reactions. For systems in which the bimolecular reaction with the G2 guest is rate limiting, the conformational rearrangement of the G2 guest required for it to pass through the host aperture will also contribute to the negative activation entropy.

(34) It was not possible to measure volumes of activation for PEt_4^+ and NEt_4^+ due to the temperature limitations of the variable pressure NMR probe.

(35) A positive volume of activation would also be expected for the bond-rupture mechanism, in which one ligand partially dissociates to open up a large host portal for guest egress. The volumes of activation for this mechanism, however, should be independent of guest size.

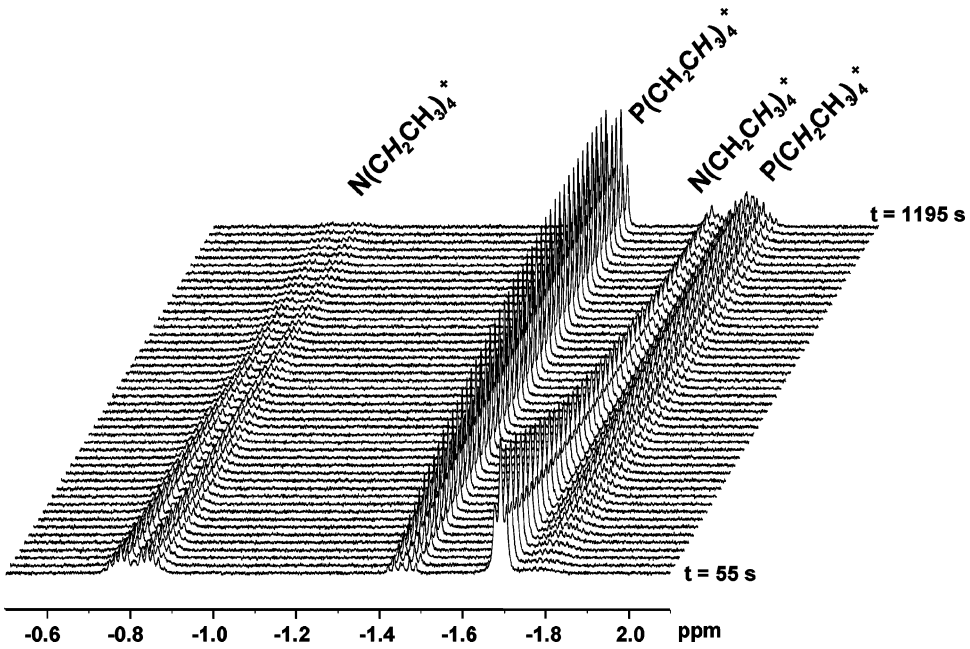

Figure 7. ^{1}H NMR (500 MHz, D_2O) spectra following the exchange of guests PEt_4^+ for NEt_4^+ in the $[Ga_4L_6]^{12-}$ host. (0.5 M KCl, pD > 12, T = 23 °C).

between the two $\Delta V^‡$ values is remarkable in that it reflects the greater degree to which the NPr_4^+ guest distends the equilibrium assembly structure as compared to the more streamlined $NMe_2Pr_2^+$, therefore confirming the proposed mechanistic model.

It is worth noting that, in many cases, reactions characterized by negative $\Delta S^‡$ also demonstrate negative $\Delta V^‡$ values. For example, in coordination chemistry associative ligand exchange mechanisms produce a compact transition state structure in which the metal complex and incoming ligand are held in close proximity, yielding a negative volume of activation and a negative entropy of activation. On the other hand, dissociative ligand exchange mechanisms are usually characterized by positive $\Delta S^‡$ and $\Delta V^‡$ values.[36] However, these scenarios are not imperative since there is no direct thermodynamic link between these activation parameters. There are a number of examples where activation entropies and activation volumes tend to go in the opposite direction especially when the activation entropy has a low absolute value.[37] In such cases each of the parameters reflects specific structural and/or solvational changes that occur on going to the transition state of the process. In the present case, the orientation and proper folding of the existing or entering guest dominates the entropic activation parameter, while the expansion of the host structure (and thereby its solvation shell and associated counterions) contributes to a positive volume of activation.

Guest Displacement Reactions. Selection of suitable guest exchange systems in which to follow the displacement of an initially encapsulated guest (G1) by a second guest species (G2) requires consideration of G1 guest binding thermodynamics. In addition the binding affinity of the G2 guest must also be sufficient to drive the exchange reaction. Displacement of NEt_4^+ by PEt_4^+ meets these criteria and proved to be a fruitful system to study. ^{1}H NMR spectra for a typical exchange reaction are shown in Figure 7. These spectra illustrate the strongly upfield shifted ^{1}H resonances of guest species, which are characteristic of encapsulation.[19] The resonances for the corresponding "free" guest populations appear downfield in the aliphatic region of the spectra.

The encapsulated and well-resolved N*CH*$_2$ and P*CH*$_3$ resonances are followed to determine the concentration of each encapsulated species with time. Treatment of the guest exchange data indicated that a pseudo first-order model could be applied, when the concentration of the new guest (here PEt_4^+) was in sufficient excess. Under these flooding conditions, the reaction is first order with respect to the tetrahedral assembly. Kinetic traces from a typical data set are shown in Figure 8, along with the first-order fitting.[38]

Experiments were conducted to test the effect of the concentration of the displacing guest (G2) on the rate of the reaction. The same reaction was repeated several times, with the concentration of the assembly and of the initial guest (G1) held constant at eight equivalents, while the G2 concentration was varied. Rate data from these experiments reveal no dependence on the G2 concentration (Figure 9), supporting a model in which the egress of the initial guest is rate determining. An egress-limited mechanism is also consistent with the observation that the displacement of a very large guest ($CoCp^*_2^+$) dramatically inhibits guest exchange.[18]

Role of Exterior Countercations. Experiments in which the concentration of the initial guest was varied were also conducted to probe the effect observed in the initial PEt_4^+ for NEt_4^+ exchange. A series of solutions was prepared, varying the concentration of NEt_4^+ (G1), while holding the concentration

(36) van Eldik, R.; Dücker-Benfer, C.; Thaler, F. *Adv. Inorg. Chem.* **2000**, *49*, 1−58. van Eldik, R.; Hubbard, C. D. In *High-Pressure Chemistry: Synthetic, Mechanistic and Supercritical Applications*; van Eldik, R., Klärner, F.-G., Eds.; VCH−Wiley: Weinheim, Germany, 2002; pp 3−40. van Eldik, R.; Hubbard, C. D. In *Chemistry at Extreme Conditions*; Riad Manaa, M., Ed.; Elsevier: Amsterdam, 2005; pp 109−164. Franke, A.; Stochel, G.; Jung, C.; van Eldik, R. *J. Am. Chem. Soc.* **2004**, *126*, 4181−4191.

(37) Laverman, L. E.; Wanat, A.; Oszajca, J.; Stochel, G.; Ford, P. C.; van Eldik, R. *J. Am. Chem. Soc.* **2001**, *123*, 285−293. Wanat, A.; Schneppensieper, T.; Stochel, G.; van Eldik, R.; Bill, E.; Wieghardt, K. *Inorg. Chem.* **2002**, *41*, 4−10. Schneppensieper, T.; Wanat, A.; Stochel, G.; van Eldik, R. *Inorg. Chem.* **2002**, *41*, 2565−2573.

(38) The reverse reaction, NEt_4^+ for PEt_4^+ exchange, produces similar kinetic behavior (Supporting Information).

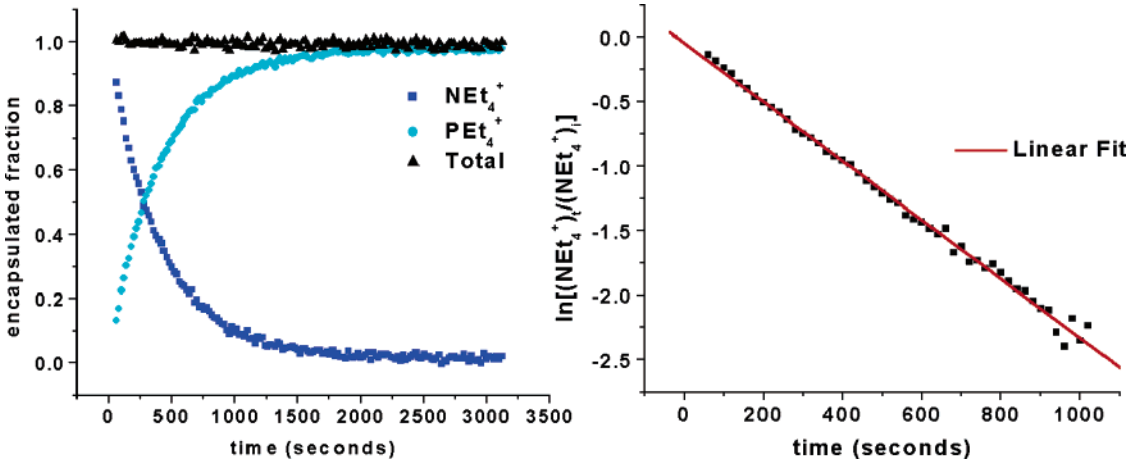

Figure 8. Kinetic traces from the displacement of NEt_4^+ by PEt_4^+. The data fit a pseudo-first-order model.

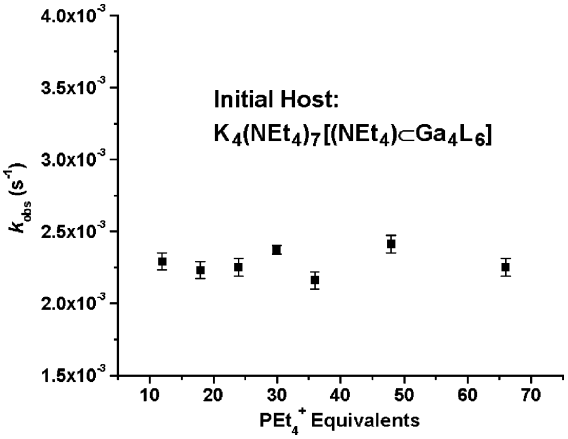

Figure 9. Displacement of NEt_4^+ by PEt_4^+ in $[Ga_4L_6]^{12-}$ shows no dependence on the PEt_4^+ concentration (G2). $[Ga_4L_6]^{12-} = 5.3$ mM; $[NEt_4^+] = 42$ mM; $[PEt_4^+] = 64-350$ mM.

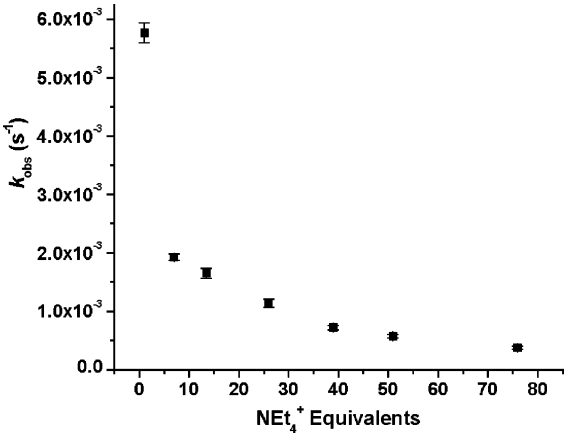

Figure 10. Increasing NEt_4^+ (G1) concentrations inhibit the PEt_4^+ for NEt_4^+ exchange in the $[(NEt_4^+)\subset Ga_4L_6]^{11-}$ host. $[NEt_4^+] = 5.4-404$ mM, $[PEt_4^+] = 64$ mM.

of the tetrahedral assembly and the concentration of the incoming guest, PEt_4^+ (G2), constant. Here, increasing concentrations of the initial guest species, NEt_4^+, inhibit the rate of PEt_4^+ for NEt_4^+ exchange (Figure 10).

The inhibition of the guest exchange rate by increased initial guest (G1) concentrations is not surprising and might be understood by invoking the thermodynamic ground state effects. Just as strongly binding guests stabilize the initial host−guest complex relative to a deformed host transition state, so can an increased G1 concentration. One might also envision that increased G1 concentrations increase the rate of G1 re-encapsulation, the k_{-1} reaction, which will lead to a decrease in the observed rate constant based on the mechanism suggested in Figure 3.

However, variation of the G2 concentration at low G1 concentrations sheds a different light on the role of nonencapsulated or "free" guest species. When the PEt_4^+ for NEt_4^+ reaction is followed in systems starting with a 1:1 $NEt_4^+/[Ga_4L_6]^{12-}$ ratio, increasing G2 (PEt_4^+) concentrations are found to *inhibit* the PEt_4^+ for NEt_4^+ exchange reaction (Figure 11)! Taken together, the G1 and G2 inhibition results in addition to the previously noted guest inhibition of self-exchange reactions point to the significance of the "free" guest species and the chemistry of the host exterior.[39] Exterior, or exohedral, guests may change the dynamics of the host itself and thereby affect guest exchange reactions.

Unencapsulated guest species are often considered to be "free" in solution; yet this may be an overly simplistic view of the solution chemistry. Other host−guest systems point to the significance of exterior counterions (or "exohedral guests")[40] in guest dynamics,[16,40,41] and previous NMR and calorimetry experiments point to significant interactions between cations and the M_4L_6 assembly exterior.[20,27] Cation-π interactions between six exohedral NEt_4^+ cations and the naphthyl rings of each ligand in the $K_5(NEt_4)_6[(NEt_4)\subset Fe_4L_6]$ crystal structure are highlighted in Figure 12.[20]

The G1 and G2 inhibition results support the idea that exohedral guest interactions inhibit guest egress, perhaps by impeding the required flexing of the host structure necessary to dilate a host aperture for guest passage. To probe the effect of exterior host−guest interactions, attempts were made to saturate the exohedral "sites" with an innocent and smaller cation. In this strategy, guest exchange in the host cavity should be relatively unaffected, while exterior host−guest interactions

(39) The G2 inhibition effect was also observed in the reverse NEt_4^+ for PEt_4^+ reaction (Supporting Information), although the stronger binding of the PEt_4^+ guest limited the extent to which this reaction was studied. Both G1 and G2 inhibition effects were also observed in PEt_4^+ for NEt_4^+ exchange reactions in the $[Al_4L_6]^{12-}$ host.

(40) Saalfrank, R. W.; Demleitner, B.; Glaser, H.; Maid, H.; Reihs, S.; Bauer, W.; Maluenga, M.; Hampel, F.; Teichert, M.; Krautscheid, H. *Eur. J. Inorg. Chem.* **2003**, 822−829.
(41) Márquez, C.; Hudgins, R. R.; Nau, W. M. *J. Am. Chem. Soc.* **2004**, *126*, 5806−5816.

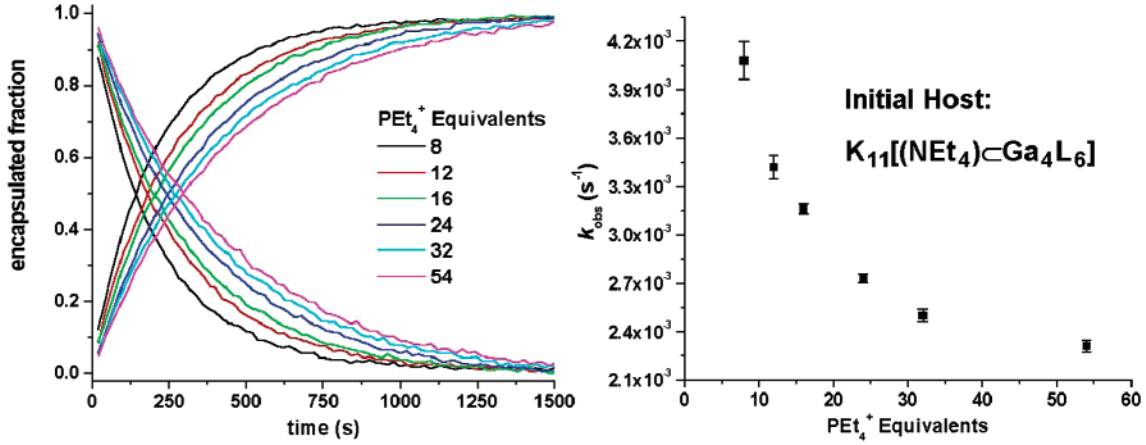

Figure 11. In systems with low G1−host ratios (here 1 NEt_4^+: 1 $[Ga_4L_6]^{12-}$), G2 inhibition is observed. *Increasing* concentrations of the displacing G2 guest, PEt_4^+ lead to *decreasing* rates of PEt_4^+ for NEt_4^+ exchange. $[K_{11}[(NEt_4)\subset Ga_4L_6]] = 5.3$ mM, $[PEt_4^+] = 43-286$ mM.

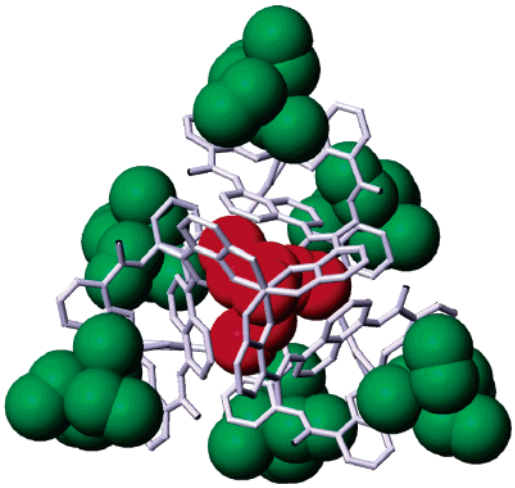

Figure 12. Exterior NEt_4^+ cations of the $K_5(NEt_4)_6[(NEt_4)\subset Fe_4L_6]$ structure interact with the aromatic naphthyl rings of the ligand backbones.

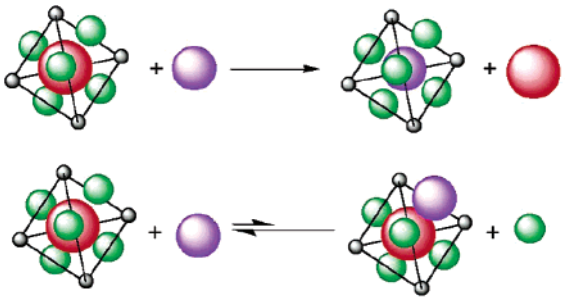

Figure 13. An exterior blocking agent should not interfere with G2 for G1 guest exchange but should inhibit exterior binding of the exchange active G1 and G2 guests.

of the G1 and G2 guests should be inhibited (Figure 13). The experimental design relies on the selection of an exterior blocking agent with a competitive affinity for the host exterior but a negligible affinity for the host interior.

Tetramethylammonium interacts significantly with the host exterior but exhibits very weak binding to the host interior (log $K = 1.5$) and was therefore chosen as the exterior blocking agent. In addition, the smaller size of NMe_4^+ may change the effect of exohedral binding on the host dynamics. A series of PEt_4^+ for NEt_4^+ guest exchange experiments were conducted in which the concentration of NMe_4^+ was varied in order to explore the effect of exterior site saturation. In each experiment

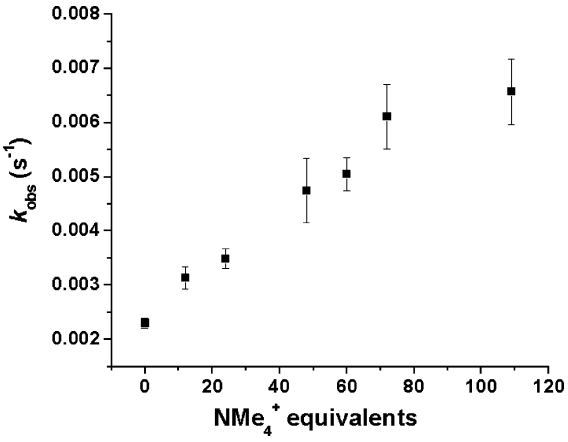

Figure 14. PEt_4^+ for NEt_4^+ guest exchange rate in $[Ga_4L_6]^{12-}$ increases with increasing concentration of the NMe_4^+ exterior blocking agent. Error bars represent 3σ as determined from the linear first-order fits.

the total salt concentration was held constant by the addition of KCl. The rate data for these experiments display an increase in the PEt_4^+ for NEt_4^+ guest exchange rate with increasing NMe_4^+ concentration (Figure 14).

The variable $[NMe_4^+]$ experiment points again to the inhibitory effect of G1 and G2 exohedral guests on the exchange of encapsulated (or endohedral) guest species in the host cavity. Exohedral guests may provide a protective shell around the host, impacting host flexibility and thereby guest exchange dynamics.[42] When the NEt_4^+ and PEt_4^+ exterior interactions are inhibited by a smaller NMe_4^+ guest, the resulting $(NMe_4)_6[Ga_4L_6]^{6-}$ host appears to be better able to accommodate guest egress and ingress. In combination with the G1 and G2 inhibition results, the NMe_4^+ blocking experiment demonstrates the kinetic significance of exterior host−guest interactions. Importantly, the exohedral guest interactions of the M_4L_6 host have also been implicated in encapsulated reaction chemistry,[43] and one might imagine controlling the reactivity of an encapsulated substrate by modulating the exohedral host interactions.

(42) Other ion pairing effects can be envisioned. For example, alkali cations are often found ion paired to the negatively charged catecholate caps of ML_3 complexes. Large ammonium (or phosphonium) cation concentrations might interfere with this interaction thereby impacting the host dynamics. Additionally, interaction of the ammonium cations with the catecholate cap may itself be a critical parameter to host dynamics.

(43) Leung, D. H.; Bergman, R. G.; Raymond, K. N. Unpublished results. Fiedler, D.; van Halbeek, H.; Bergman, R. G.; Raymond, K. N. Unpublished results.

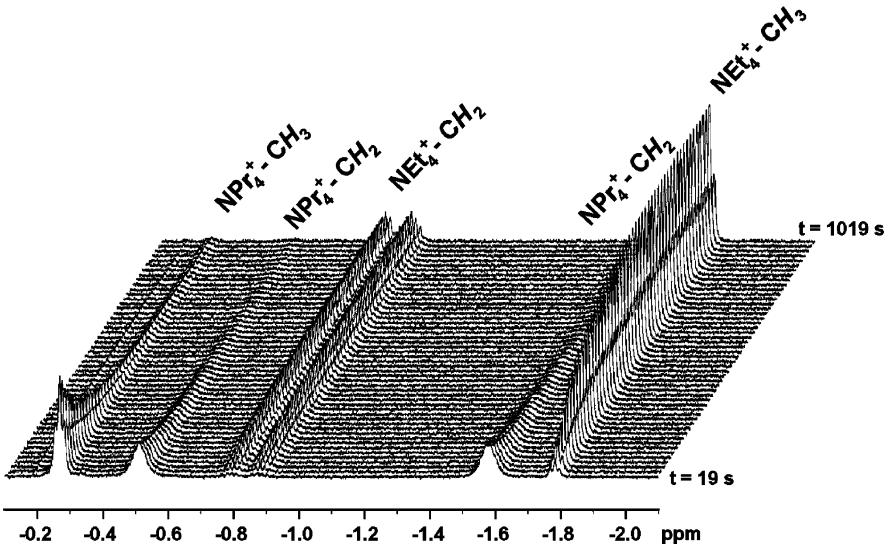

Figure 15. ^{1}H NMR spectra (500 MHz, D_2O) following the exchange of NEt_4^+ for NPr_4^+ in $[Ga_4L_6]^{12-}$. The chemical shift of methyl protons of the encapsulated NPr_4^+ shifts with the composition of the exterior cations, and thus this spectrum is different from that of Figure 5.

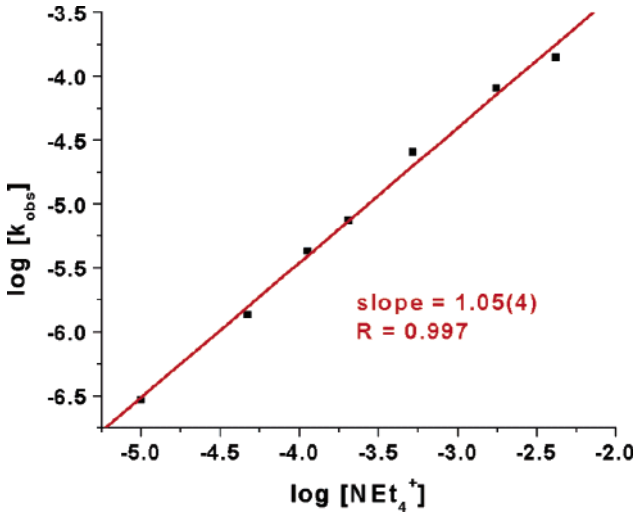

Figure 16. NEt_4^+ (5.5−66mM) for NPr_4^+ (200 mM) exchange in $[Ga_4L_6]^{12}$ (5.4 mM): $\log[k_{obs}]$ vs $\log[NEt_4^+]$ reveals a first-order dependence of the rate expression on [G2].

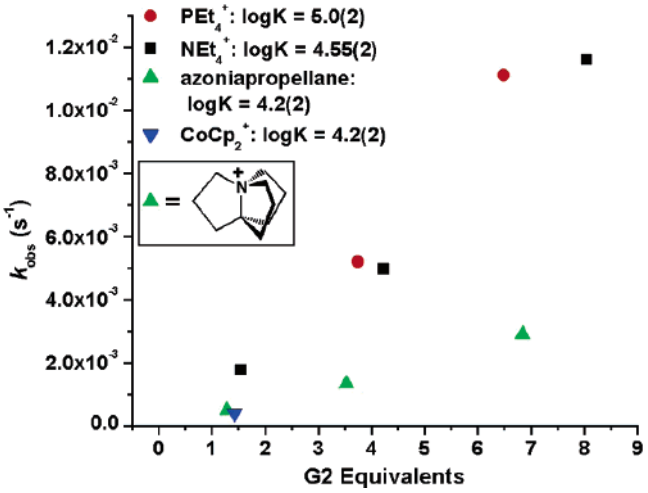

Figure 17. Displacement rate of NPr_4^+ varies with the identity of the G2 guest. Stronger binding guests produce faster rates.[19,22,26,27,44] $[Ga_4L_6]^{12-}$ = 5.4 mM, $[NPr_4^+]$ (G1) = 167 mM. Experiments with higher ratios of $CoCp_2^+$ were not possible due to precipitation of the $CoCp_2^+$ ion-paired host.

Guest Influence on the Kinetic Model

The experiments described thus far employ strongly binding guests in guest exchange reactions and, therefore, restrict the selection of exchanging species. Yet, weakly binding guests exchange faster, also limiting the range of systems accessible to study. Large excesses of NPr_4^+ slow the exchange of NEt_4^+ for NPr_4^+ enough to be followed by NMR, and a representative series of ^{1}H NMR spectra from this exchange is shown in Figure 15.

Unlike the PEt_4^+/NEt_4^+ exchange system, the $[(NPr_4)\subset Ga_4L_6]^{11-}$ data exhibit an increase in guest exchange rates with increasing [G2] concentration, and a plot of $\log[k_{obs}]$ vs $\log[NEt_4^+]$ demonstrates the first-order dependence on [G2] in these reactions (Figure 16). Guest egress of the G1 guest, now the weakly binding NPr_4^+, no longer limits the guest exchange reaction. Instead, the bimolecular reaction of empty host and G2 guest becomes rate determining.[28]

The $[(NPr_4)\subset Ga_4L_6]^{11-}$ system also provides an opportunity to probe the sensitivity of the guest exchange kinetics to the identity of the G2 displacing guest. Rate data from the displacement of NPr_4^+ by four different guests (PEt_4^+, NEt_4^+, azoniapropellane, and cobaltacinium) are presented in Figure 17.

This series of guests indicates that stronger binding G2 guests produce faster rates of guest exchange in the $[(NPr_4)\subset Ga_4L_6]^{11-}$ system. As the G2 guest binding strength increases, the thermodynamic driving force for the exchange reaction increases, but it is not clear what effect this has on the k_2 step of the guest exchange. A stronger binding guest would inhibit the k_{-2} step (Figure 3), the dissociation of G2, and this might be factor in the observed trend. Intriguingly, however, the displacement of NPr_4^+ by $NMe_2Pr_2^+$ was too fast to measure, despite its lower binding constant. As was observed in the self-exchange experiments, the streamlined shape of $NMe_2Pr_2^+$ enhances its ability to slip into and out of the M_4L_6 host through its available apertures. Finally these results might also be indicative of differences in the exohedral affinities of the different G2 guests.

Conclusion and Summary

Kinetic study of the host−guest dynamics of the $[Ga_4L_6]^{12-}$ assembly provides substantial evidence in support of a nondissociative guest exchange mechanism. While the enthalpies of activation for guest self-exchange correlate with guest binding affinities, negative $\Delta S^{\ddagger}$ values corroborate the squeezing of guests through a tight host aperture (and the concomitant restructuring of the host and its counterions). Consequently, the largest guest examined, NPr_4^+, demonstrates a much more negative $\Delta S^{\ddagger}$ value than its smaller counterparts, PEt_4^+, NEt_4^+, and $NMe_2Pr_2^+$. Positive volumes of activation for the guest exchange process are also indicative of the distension of the guest structure involved in aperture enlargement. The more streamlined geometry of $NMe_2Pr_2^+$ as compared to NPr_4^+ is evidenced in its lower volume activation.

Guest displacement reactions emphasize the role of thermodynamic guest affinities in modulating guest exchange rates. For strongly binding guests, such as NEt_4^+ and PEt_4^+, guest release and formation of an empty host is rate limiting in exchange reactions.[28] Guest exchange is retarded by increasing initial guest concentrations, as well as by increasing G2 equivalents when G1 levels are low. Thus, the total guest (G1 + G2) concentration and combined affinity for the host exterior influences host dynamics. In this model, exohedral guests inhibit the host's capacity to deform and thus allow guest passage through a dilated aperture. However, blocking of the exohedral guest sites by the smaller NMe_4^+ increases PEt_4^+ for NEt_4^+ exchange rates, perhaps by facilitating greater host flexibility. Finally, when a more weakly binding initial guest occupies the host cavity (NPr_4^+), guest exchange rate dependence on the displacing, G2 guest concentration is observed in addition to a dependence on the binding affinity of the G2 guest.

These studies add to our growing knowledge of the solution behavior of the remarkable M_4L_6 assembly and our ability to predict and control its functionality. Current studies defining and expanding the scope of the M_4L_6 host as a nanoscale molecular reactor already rely on the mechanistic and kinetic parameters of its guest exchange chemistry to probe the details and boundaries of encapsulated reactions. For example, in an encapsulated reaction cycle which reaction steps really occur in the inner-phase and which are exposed to the bulk solution? Recent studies already point to the influence of exohedral guest interactions on substrate reactivity.[43] The complex solution behavior of supramolecular structures continues to provide new opportunities for transforming and controlling "inner-phase" chemistry (and perhaps "outer-phase" as well).

Experimental Section

General. Reagents were obtained from commercial suppliers and used without further purification unless noted. Et_4NCl was precipitated from ethanol, filtered, and rigorously dried. $[CoCp_2]Cl$ was precipitated with ether from a chilled acetonitrile solution of $[CoCp_2]PF_6$ and NBu_4Cl, filtered, and rigorously dried. Ligand H_4L, complexes $K_n[NEt_4]_{11-n}[(NEt_4)\subset Ga_4L_6]$ were prepared as previously reported.[20] NMR spectra were obtained using a 500 MHz Bruker DRX-500 spectrometer unless otherwise specified. ^1H NMR shifts are reported as δ in ppm relative to residual protonated solvent resonances. Mass spectra were recorded at the UCB Mass Spectrometry Facility, and elemental analyses were performed at the UCB Analytical Facility.

Metal Complex Syntheses. A. $K_{11}[(PEt_4)\subset Ga_4L_6]$. H_4L (71.3 mg, 0.166 mmol) and PEt_4Br (6.4 mg, 0.028 mmol) were suspended in methanol (30 mL) and degassed. To this solution was added a 0.50 M methanolic solution of KOH (663 μL, 0.332 mmol), followed by $Ga(acac)_3$ (40.0 mg, 0.109 mmol). The resulting yellow solution stirred under a nitrogen atmosphere overnight. The solution volume was then reduced to approximately 2 mL, and a yellow solid was precipitated by the addition of acetone. The product was dried under vacuum at 60 °C. Yield: 76.3 mg (80.3%). ^1H NMR (500 MHz, D_2O): δ 8.07 (d, J = 7.8 Hz, 12H, Ar*H*), 7.88 (d, J = 8.5 Hz, 12H, Ar*H*), 7.36 (dd, ^3J = 8.2 Hz, ^4J = 1.4 Hz, 12H, Ar*H*), 7.14 (t, J = 8.2 Hz, 12H, Ar*H*), 6.81 (dd, ^3J = 7.4 Hz, ^4J = 1.4 Hz, 12H, Ar*H*), 6.66 (t, J = 7.8 Hz, 12H, Ar*H*), −1.29 (dt, $^3J_{P-H}$ = 18.5 Hz, $^3J_{H-H}$ = 7.6 Hz, 12H, C*H*$_3$), −1.58 (m, 8H, C*H*$_2$). $^{13}C\{^1H\}$ NMR (100 MHz, D_2O): δ 170.3, 159.1, 155.3, 134.5, 127.1, 126.9, 119.3, 118.2, 116.1, 115.7, 115.4, 115.3, 9.3 (d, $^1J_{C-P}$ = 48.4 Hz), 3.5 (d, $^2J_{C-P}$ = 5.3 Hz). $^{31}P\{^1H\}$ NMR (160 MHz, D_2O): δ 34.8 (addition of more than 1 equiv of PEt_4^+ produces a second resonance at 38.7). MS (ES-): *m*/*z* 1048.1 ($K_4H_4[(PEt_4)\subset Ga_4L_6]^{3-}$), 795.3 ($[(PEt_4)\subset Ga_4L_6]^{3-}$). Anal. Calcd (found) for $K_{11}Ga_4C_{152}H_{104}N_{12}O_{36}P\cdot 4H_2O$: C, 52.36 (52.33); H, 3.24 (3.05); N, 4.82 (4.65).

B. $K_{10}(NPr_4)[(NPr_4)\subset Ga_4L_6]$. The complex was prepared from H_4L (66.9 mg, 0.155 mmol), NPr_4Br (28.0 mg, 0.105 mmol), $Ga(acac)_3$ (37.3 mg, 0.102 mmol), and a 0.5 M methanolic KOH solution (622 μL, 0.311 mmol), following a procedure analogous to that described for $K_{11}[(PEt_4)\subset Ga_4L_6]$. Importantly, NPr_4Br must be added to the reaction solution last in order to avoid precipitation of the deprotonated ligand. The product was isolated as a yellow powder. Yield: 84.4 mg. ^1H NMR (500 MHz, D_2O): δ 8.07 (d, J = 7.7 Hz, 12H, Ar*H*), 7.74 (d, J = 8.5 Hz, 12H, Ar*H*), 7.30 (d, J = 8.1 Hz, 12H, Ar*H*), 6.89 (t, J = 8.1 Hz, 12H, Ar*H*), 6.73 (d, J = 7.0 Hz, 12 H, Ar*H*), 6.58 (t, J = 7.8 Hz, 12 H, Ar*H*), 2.48 (br m, 8H, C*H*$_2$), 1.16 (br m, 8H, C*H*$_2$), 0.66 (t, J = 6.9 Hz, 12H, C*H*$_2$), −0.23 (br m, 4H, CH*H*), −0.38 (br m, 4H, CH*H*), −0.68 (t, J = 6.8 Hz, 12 H, C*H*$_3$), −1.29 (br m, 4H, CH*H*), −1.45 (br m, 4H, CH*H*) (methylene resonances are diastereotopic in the chiral tetrahedron and appear separately). $^{13}C\{^1H\}$ NMR (100 MHz, D_2O): δ 169.8, 158.8, 155.0, 134.4, 126.8, 126.7, 119.2, 118.1, 116.0, 115.3, 115.1, 115.1, 59.9, 58.2, 15.0, 13.7, 11.2, 10.4. Anal. Calcd (found) for $K_{10}Ga_4C_{168}H_{140}N_{14}O_{36}$: C, 56.04 (55.92); H, 3.92 (4.06); N, 5.45 (5.26).

C. $K_8(NEt_4)_3[(NEt_4)\subset Al_4L_6]$. The complex was prepared from H_4L (75.7 mg, 0.176 mmol), NEt_4Br (25.1 mg, 0.119 mmol), $Al(acac)_3$ (37.9 mg, 0.117 mmol), and a 0.5 M methanolic KOH solution (703 μL, 0.352 mmol), following a procedure analogous to that described for $K_{11}[(PEt_4)\subset Ga_4L_6]$. The product was isolated as a yellow powder. Yield: 80.4 mg (77.8%). ^1H NMR (500 MHz, D_2O): δ 8.08 (d, J = 7.8 Hz, 12H, Ar*H*), 7.88 (d, J = 8.6 Hz, 12H, Ar*H*); 7.30 (dd, ^3J = 8.2 Hz, ^4J = 1.6 Hz, 12H, Ar*H*), 7.19 (t, J = 8.2 Hz, 12H, Ar*H*), 6.71 (dd, ^3J = 7.3 Hz, ^4J = 1.6 Hz, 12H, Ar*H*), 6.64 (t, J = 7.8 Hz, 12H, Ar*H*); 2.63 (q, J = 7.2 Hz, 24H, C*H*$_2$), 0.83 (t, J = 7.1 Hz, 36H, C*H*$_3$); −0.68 (q, J = 7.2 Hz, 8H, C*H*$_2$); −1.55 (t, J = 7.2 Hz, 12H, C*H*$_3$). ^{13}C NMR (125 MHz, D_2O): δ 170.3, 160.0, 156.4, 134.5, 127.1, 119.4, 118.1, 115.8, 115.6, 114.8, 114.7, 52.2, 50.8, 6.8, 4.8. MS (ES-): *m*/*z* 1127.3 ($K_5(NEt_4)_3[(NEt_4\subset Al_4L_6]^{3-}$), 1114.7 ($K_4H(NEt_4)_3[(NEt_4\subset Al_4L_6]^{3-}$), 1089.4 ($K_2H_6(NEt_4)_3[(NEt_4\subset Al_4L_6]^{3-}$), 826.5 ($K_3H(NEt_4)_3[(NEt_4r\subset Al_4L_6]^{4-}$), 816.8 ($K_2H_2(NEt_4)_3[(NEt_4\subset Al_4L_6]^{4-}$). Anal. Calcd (found) for $K_8Al_4C_{176}H_{164}N_{16}O_{36}\cdot 2H_2O$: C, 59.78 (59.84); H, 4.79 (4.55); N, 6.34 (6.15).

D. $K_8(PEt_4)_3[(PEt_4)\subset Al_4L_6]$. The complex was prepared from H_4L (75.2 mg, 0.175 mmol), PEt_4Br (26.0 mg, 0.115 mmol), $Al(acac)_3$ (37.2 mg, 0.115 mmol), and a 0.5 M methanolic KOH solution (699 μL, 0.350 mmol), following a procedure analogous to that described for $K_{11}[(PEt_4)\subset Ga_4L_6]$. The product was isolated as a yellow powder. Yield: 91.8 mg. ^1H NMR (500 MHz, D_2O): δ 8.12 (d, J = 7.6 Hz, 12H, Ar*H*), 7.88 (d, J = 8.4 Hz, 12H, Ar*H*), 7.32 (dd, ^3J = 8.1 Hz, ^4J = 1.4 Hz, 12H, Ar*H*), 7.18 (t, J = 8.0 Hz, 12H, Ar*H*), 6.72 (dd, ^3J = 7.3 Hz, 12H, Ar*H*), 6.65 (t, J = 7.8 Hz, 12H, Ar*H*), 1.58 (br, 24H, C*H*$_2$), 0.69 (br m, 36H, C*H*$_3$), −1.29 (dt, $^3J_{P-H}$ = 18.1 Hz, $^3J_{H-H}$ = 7.8 Hz, 12H, C*H*$_3$), −1.66 (m, 8H, C*H*$_2$). $^{13}C\{^1H\}$ NMR (100 MHz, D_2O):

δ 170.3, 160.0, 156.4, 134.5, 127.1, 127.0, 119.4, 118.2, 115.8, 115.6, 114.8,, 10.7 (d, $J_{C-P} = 49.5$ Hz), 9.3 (d, $^1J_{C-P} = 48.1$ Hz), 4.9 (d, $^2J_{C-P} = 5.5$ Hz), 3.7 (d, $J_{C-P} = 5.6$ Hz). $^{31}P\{H^1\}$ NMR (160 MHz, D_2O): δ 38.9, 34.7. Anal. Calcd. (found) for $K_8Al_4C_{176}H_{164}N_{12}O_{36}P_4 \cdot 2H_2O$: C 58.66 (58.66); H 4.70 (4.36); N 4.66 (4.58).

Kinetic Experiments. All solutions were prepared in D_2O (0.5 M KCl, 0.01 M NaOD) with pD > 12. Reaction solutions were prepared in screw top NMR tubes equipped with Teflon lined rubber septa. All spectra were recorded on a Bruker DRX 500 spectrometer. Samples were equilibrated to 22 ± 0.1 °C in the spectrometer probe prior to injection of the G2 solution. After approximately 10 min of temperature equilibration, the sample tube was ejected. The G2 solution was injected through the NMR tube septum with a glass airtight Hamilton microsyringe, and the sample tube was inverted several times to ensure proper mixing between the reacting solutions. The tube was then returned to the probe, and data collection was initiated. The delay between solution mixing and the acquisition initiation was recorded and included in the data analysis. One-scan ^1H NMR spectra were recorded at a set interval with an automated routine. After acquisition, the pD of each sample was measured. The standard conversion for the pH calibrated electrode of pD = pH + 0.4 was employed.[45] Further details for each experiment are provided in the Supporting Information.

Selective Inversion Recovery Experiments. These ^1H NMR experiments were performed on the DRX-500. Temperature calibration was accomplished using an ethylene glycol or methanol standard. The intensity data were fit with the CIFIT program. Each experimental solution was prepared in a medium walled NMR tube from the same stock solution of $K_8[NMe_4]_3[(NMe_4)\subset Ga_4L_6]$. All solutions were prepared in D_2O containing 0.5 M KCl and 0.01 M NaOD. For each sample 400 μL of a 8.0 mM $K_8[NMe_4]_3[(NMe_4)\subset Ga_4L_6]$ solution was combined with 50 μL of a 290 mM solution of the guest compound (PEt_4Br, NEt_4Cl, NMe_2Pr_2I, or NPr_4Br) and 150 μL of the buffer solution. Each experimental solution was degassed and sealed under an atmosphere of nitrogen. In a typical experiment approximately 30 spectra were collected with the delay between selective inversion and spectrum acquisition ranging from 10 μs to 8 s. For NEt_4^+ and PEt_4^+, experiments were performed at 313.5, 329.8, 341.1, and 367.2 K. For $NMe_2Pr_2^+$ and NPr_4^+, experiments were performed at 278.9, 288.6, 298.7, and 309.9 K.

Variable Pressure Experiments. Variable-pressure FT ^1H NMR spectra were recorded at 400 MHz on a Bruker Avance DRX 400WB spectrometer at the University of Erlangen-Nürnberg, Germany. A homemade high-pressure probe[46] was used for the variable-pressure experiments performed at the selected temperatures in the pressure range 1−160 MPa. The sample was placed in a standard 5 mm NMR tube cut to a length of 45 mm. The pressure was transmitted to the sample by a movable macor piston, and the temperature was controlled as described elsewhere.[46] The selective inversion recovery technique was employed to determine the self-exchange rate constants as a function of pressure.

Acknowledgment. We thank D. H. Leung for helpful discussions, and R. Nunlist and H. van Halbeek at the UCB NMR facility for assistance in setting up the SIR experiment. This work was supported by NSF Grant CHE-9709621 (K.N.R.), the Deutsche Forschungsgemeinschaft through SFB 583 (R.v.E.), and the Alexander von Humboldt Foundation (G.S.).

Note Added after ASAP Publication. After this paper was published ASAP on January 4, 2006, a composition error affecting the right-hand side of eq 1 was corrected. The corrected version was published ASAP January 9, 2006.

Supporting Information Available: Kinetic plots, tables of guest exchange (and self-exchange) rate constants, Eyring plots, and further experimental details. This material is available free of charge via the Internet at http://pubs.acs.org.

JA056556+

(44) The binding constant for azoniapropellane was determined by ^1H NMR relative to that of NEt_4^+.
(45) Perrin, D. D.; Dempsey, B. *Buffers for pH and Metal Ion Control*; Chapman and Hall: London, 1974.
(46) Zahl, A.; Igel, P.; Weller, M.; van Eldik, R. *Rev. Sci. Instrum.* **2004**, *75*, 3152−3157.